AIMS Mathematics, 11(4): 11173–11193.
DOI: 10.3934/math.2026460
Received: 20 February 2026
Revised: 06 April 2026
Accepted: 14 April 2026
Published: 21 April 2026

https://www.aimspress.com/journal/Math

Research article

Event-triggered synchronization for delayed dynamic complex networks via impulsive control strategy

Jiayi Cai[1,2,*], **Jiang Yu**[1,2], **Ze You**[1,2,*] **and Chenglin Jing**[1,2]

[1] School of Mathematics and Statistics, Guizhou University of Finance and Economics, Guiyang, 550025, Guizhou, China

[2] School of Big Data Statistics, Guizhou University of Finance and Economics, Guiyang, 550025, Guizhou, China

* **Correspondence:** Email: caijiayi_gufe@163.com, youze_gufe@163.com.

Abstract: This paper investigates the problem of event-triggered impulsive synchronization control for a class of hybrid delayed dynamical complex networks. Based on the Lyapunov function method, two control strategies—distributed event-triggered impulsive control and event-triggered pinning impulsive control—are proposed to guarantee synchronization of complex networks. The first strategy does not require prior knowledge of the network topology, thereby greatly reducing implementation difficulty. The second strategy controls only a subset of nodes in the network, which significantly reduces the consumption of control resources. Several sufficient conditions are established to reveal the potential relationships among the event-triggered mechanisms, control input, and impulsive action. In addition, the proposed event-triggered mechanisms can effectively exclude Zeno behavior. Finally, some numerical examples are provided to verify the effectiveness of the theoretical results for the synchronization of delayed dynamic complex networks.

Keywords: event-triggered impulsive; distributed control; pinning synchronization; Zeno behavior
Mathematics Subject Classification: 93C27

1. Introduction

In recent years, synchronization control of complex networks has attracted considerable attention in mathematics, computer science, physics, and related fields; see [1–3] and the references therein. Synchronization refers to a process in which two or more systems interact with one another in addition to their individual evolution, such that their states gradually converge under coupling when certain conditions are satisfied [4, 5]. For systems that cannot achieve synchronization through their inherent dynamics and coupling alone, control inputs are introduced to enforce synchronization. Among various

control strategies, impulsive control has been widely studied because of its simple structure, low implementation cost, and strong robustness. In particular, impulsive control permits discontinuous control actions, making it suitable for systems in which continuous control inputs are infeasible or unavailable. As a result, it offers broader applicability than conventional continuous control schemes. To date, a substantial body of literature has been devoted to impulsive control; see [6–8] and the references therein. However, in most existing studies, impulsive control is implemented at prespecified impulsive instants, which may lead to unnecessary resource consumption. In practical applications, improving resource utilization efficiency is essential for guaranteeing the desired synchronization performance while reducing control expenditure [9, 10].

To improve the efficiency of impulsive control, event-triggered impulsive control has been extensively investigated in recent years; see [11,12]. The main idea of this approach is that an impulsive signal is applied only when the system dynamics violate a prespecified trigger condition. Unlike time-triggered impulsive control, the number of impulses is not predetermined, and the impulsive controller is activated only when the triggering condition is satisfied, thereby substantially reducing the consumption of control resources [13, 14]. Compared with conventional event-triggered control based on zero-order hold, event-triggered impulsive control also requires real-time monitoring of the system state; however, its control action is instantaneous at each triggering instant, and no control input is imposed between two consecutive impulse instants. Consequently, the communication burden can be significantly reduced. To date, various event-triggered impulsive control strategies have been applied to a wide range of control problems. For example, [15] investigated the application of event-triggered impulsive control to the synchronization of multiple neural networks and discussed event-triggered impulsive synchronization in complex dynamical networks with leader. Peng et al. [16] employed event-triggered impulsive control to study synchronization in leader-following coupled dynamical networks. References [17] and [18] addressed event-triggered impulsive control for first-order and second-order multi-agent systems, respectively. However, in previous studies on event-triggered impulsive control, implementation of the reported results generally required prior knowledge of the network topology, which is difficult to obtain in some practical scenarios. In addition, for networks with low synchronization performance requirements, or for networks in which controllers can only be installed at a subset of nodes, it remains necessary to further reduce control resource consumption and develop suitable event-triggered impulsive control schemes. Therefore, overcoming these difficulties and filling these theoretical gaps constitute the main motivation of this paper.

Time delays are ubiquitous in real-world physical networks. If not properly addressed, they may degrade control performance or even destabilize the system [19, 20]. Therefore, the study of control methods for delayed networks is motivated by both theoretical challenges and practical demands. On the one hand, time-triggered impulsive control for delayed networks has been extensively studied; see, for example, [21, 22]. On the other hand, it is well known that one of the key issues in the design of event-triggered mechanisms is the exclusion of Zeno behavior, that is, infinitely many triggering events occurring within a finite time interval. The presence of time delays further complicates this task, because estimating delayed state information while simultaneously excluding Zeno behavior is highly challenging. Nevertheless, some progress has been made in recent years on event-triggered control strategies for delayed systems; see [23–25]. More recently, event-triggered impulsive control for delayed systems has also attracted increasing attention. In [12], a suitable event-triggered impulsive control strategy was developed to guarantee global weak exponential stability for

a delayed system. However, this strategy cannot be directly extended to delayed networks, mainly because the coupling among network nodes further increases the difficulty of extracting delayed state information while excluding Zeno behavior. Although event-triggered impulsive control strategies for delay-free networks have been widely investigated, corresponding studies for delayed networks remain relatively limited. These considerations motivate the present study. The primary contributions of this paper are summarized as follows:

(1) Distributed event-triggered impulsive control strategy: A novel distributed event-triggered impulsive control method is proposed in the first control strategy. Unlike most existing studies that depend on the global network topology, the proposed approach requires only information from neighboring nodes. This use of localized information substantially improves the feasibility and scalability of the control strategy and makes it more suitable for large-scale networks. By reducing reliance on global network information, the proposed method is more practical for applications in which complete network information is unavailable or expensive to obtain.

(2) Pinning control integrated with event-triggered impulsive control: In the second control strategy, pinning control is incorporated into the event-triggered impulsive control framework. This integration enables synchronization to be achieved by controlling only a subset of nodes rather than the entire network. Consequently, control resource consumption is further reduced, which improves the efficiency of the strategy. This approach is particularly suitable for networks with limited control capability or strict resource constraints.

(3) Synchronization conditions and practical implementation: Several sufficient conditions are derived to ensure synchronization of complex networks, and these conditions are simple and convenient to implement. They establish explicit relationships between impulse intervals and key factors of network dynamics, including continuous-time dynamics, topology, and event-triggered mechanisms. By clearly characterizing these relationships, the obtained results provide useful guidance for the design and optimization of event-triggered impulsive control strategies. The simplicity of the proposed conditions also supports their application to a broad class of complex network scenarios. Taken together, these contributions advance the study of complex network control by addressing important issues related to feasibility, resource efficiency, and practical implementation. The proposed strategies not only improve the effectiveness of event-triggered impulsive control but also provide a basis for future research on distributed and resource-efficient control methods.

These contributions collectively advance the field of complex network control by addressing critical challenges related to feasibility, resource efficiency, and practical implementation. Our proposed strategies not only improve the performance of event-triggered impulsive control but also provide a foundation for future research in distributed and resource-efficient control methodologies.

Notations: Let $\mathbb{R}$ denote the set of real numbers and $\mathbb{R}^+$represent the set of positive real numbers. The notation $\mathbb{R}^n$ denotes the n-dimensional real vector space, while $\mathbb{R}^{n\times m}$ represents the space of $n\times m$-dimensional real matrices. Both spaces are equipped with the Euclidean norm, denoted by $\|\cdot\|$. For a given matrix Q, $\lambda_{\max}(Q)$ and $\lambda_{\min}(Q)$ refer to its maximum and minimum eigenvalues, respectively.

2. Model description

The following equation describes a class of coupled complex networks composed of N dynamical nodes with hybrid time-varying delays:

$$\dot{z}_i(t) = \tilde{\phi}(t, z_i(t), z_i(t-\varrho(t))) + \sum_{j=1}^{N} g_{ij}\Gamma z_j(t-\varsigma(t)) + u_i(t), i = 1, 2, \cdots, N, \tag{2.1}$$

where $z_i(t) = (z_{i1}(t), z_{i2}(t), \cdots, z_{in}(t))^T \in \mathbb{R}^n$ is the state vector, and function $\tilde{\phi}(t, z_i(t), z_i(t-\varrho(t)))= \left[\tilde{\phi}_1(t, z_i(t), z_i(t-\varrho(t))), \cdots, \tilde{\phi}_n(t, z_i(t), z_i(t-\varrho(t)))\right]^T \in \mathbb{R}^n$. The inner coupling matrix defined as $\Gamma = \text{diag}\{\gamma_1, \gamma_2, \cdots, \gamma_n\} > 0$. $\varrho(t)$ is the transmission delay occurring inside the node satisfying $0 \le \varrho(t) \le \varrho$, and $0 \le \varsigma(t) \le \varsigma$ represents the coupled delay. Let $d = \max\{\varrho, \varsigma\}$, then the initial condition is given by $z_i(t) = \zeta_i(t)$. $G = \left(g_{ij}\right)_{N\times N}$ represents the coupling matrix of the complex network defined to satisfy diffusive coupling. Respectively, if node i can receive the information from node j, $g_{ij} > 0$, otherwise, $g_{ij} = 0$, and the diagonal elements $g_{ii} = -\sum_{j=1, j\neq i}^{N} g_{ij}$. This paper aims to synchronize each node in the coupled networks with the solution of the following nodes:

$$\dot{s}(t) = \tilde{\phi}(t, s(t), s(t-\varrho(t))),$$

where $s(t) = [s_1(t), s_2(t), \cdots, s_n(t)]^T \in \mathbb{R}^n$. Next, we will design the event-triggered mechanism and the controller to synchronize the networks.

Assumption 2.1. *The nonlinear function $\tilde{\phi}(t, x, y) : \mathbb{R}\times\mathbb{R}^n\times\mathbb{R}^n \to \mathbb{R}^n$ is supposed to satisfy the common Lipschitz condition, that is, there exist positive numbers l_1 and l_2 such that for all $x_1, x_2, y_1, y_2 \in \mathbb{R}^n$, the following condition holds:*

$$\|\tilde{\phi}(t, x_1, y_1) - \tilde{\phi}(t, x_2, y_2)\| \le l_1\|x_1 - x_2\| + l_2\|y_1 - y_2\|.$$

Definition 2.1. *[26] A network containing N nodes has a node state denoted as $z_i(t), i = 1, 2, \cdots, N$. If*

$$\lim_{t\to+\infty} \|z_i(t) - s(t)\| = 0,$$

then (2.1) could claim that the network is synchronized to $s(t)$.

3. Main results

In this section, for networks with hybrid delays, we propose two control strategies to bring the network into synchronization. Different from general impulsive control methods that require the selection of an appropriate average impulsive interval, the impulsive interval of our proposed control method is implicitly determined by an event-triggered mechanism. The derived conditions reveal the relationship between the event-triggered mechanism, the forced impulsive interval, and the control gain.

This part investigates event-triggered impulsive control from two perspectives. The first part considers a distributed event-triggered impulsive control strategy, in which all nodes independently implement an event-triggered mechanism, and each node determines its own impulsive instants based

on its local state error, without applying pinning control. The second part considers a pinning event-triggered impulsive control strategy, in which impulsive control is applied only to a subset of nodes in the network, but the event-triggered condition is designed in a centralized manner, and the triggering instants of all nodes are determined by a unified global condition. These two strategies reveal, from different aspects, the combination of event-triggered mechanisms and impulsive control.

3.1. Distributed event-triggered impulsive control strategy

We first consider imposing control on all nodes in the network by designing the following controller and event-triggered mechanism, and the impulse time of each node is independent. More specifically, the impulse time of node i is determined by the following event-triggered mechanism:

$$\begin{aligned} t_k^i &= \min\left\{\sigma_k^i, \tau_k^i\right\}, \\ \sigma_k^i &= \inf\left\{t \geq t_{k-1}^i : y_i^T(t) y_i(t) \geq a y_i^T\left(t_{k-1}^i\right) y_i\left(t_{k-1}^i\right) + b V_{i0} \mathrm{e}^{-\lambda(t-t_0)}\right\}, \end{aligned} \tag{3.1}$$

where $k \in \mathbb{Z}_+$, $a, b > 1$, $V_{i0} = \sup_{s\in[-d,0]} y_i^T(t_0+s) y_i(t_0+s)$, $y_i(t) = z_i(t) - s(t)$ denotes the error vector of node i. In particular, τ_k^i represents the forced impulsive sequence, defined as $\tau_k^i = t_{k-1}^i + \eta$ with $\eta > 0$. At the impulse time, the network is controlled by the following controller:

$$u_i(t) = \mu \sum_{k=1}^{\infty} y_i(t) \delta\left(t - t_k^i\right), \tag{3.2}$$

where the real number μ satisfies $|1+\mu| < 1$. Then the error system can be rewritten as

$$\begin{cases} \dot{y}_i(t) = \phi\left(t, y_i(t), y_i(t-\varrho(t))\right) + \sum_{j=1}^{N} g_{ij} \Gamma y_j\left(t - \varsigma(t)\right), t \neq t_k^i, \\ y_i(t_k^{i+}) = (1+\mu) y_i\left(t_k^{i-}\right), t = t_k^i, \end{cases} \tag{3.3}$$

where $\phi\left(t, y_i(t), y_i\left(t-\varrho(t)\right)\right) = \tilde{\phi}\left(t, z_i(t), z_i\left(t-\varrho(t)\right)\right) - \tilde{\phi}\left(t, s_i(t), s_i\left(t-\varrho(t)\right)\right)$.

In event-triggered mechanisms (3.1), the impulsive sequence for node i is determined by two parts, the time sequence when the event is triggered and the forced impulsive sequence that we set. Due to the inability of the threshold to spontaneously converge to zero may result in events not being triggered, thus only guaranteeing boundedness of the error vector and not synchronization. For this reason, forced sequences $\{\sigma_k^i\}$ are introduced, where events are forced to be triggered once when they do not occur for a long time, thus avoiding the above situation. To make the narrative more convenient, we merge the impulsive time series $\{t_k^i\}_{k=1}^{+\infty}$ of all nodes in chronological order to form a new time series $\{t_k\}_{k=1}^{+\infty}$, i.e., $\{t_k\} = \{t_k^i : i = 1, 2, \cdots, N, k \in \mathbb{N}^+\}$.

Theorem 3.1. *Under the conditions of Assumption 2.1, if there exist constants $a, b > 1$ and $\eta, \lambda > 0$ such that the inequality $\lambda\eta + \ln\left[a(1+\mu)^2\right] < 0$ holds, then the complex network described by (2.1), equipped with the event-triggered mechanism (3.1) and the controller (3.2), achieves global synchronization with the target trajectory $s(t)$. Furthermore, it is guaranteed that no Zeno behavior occurs in the system.*

Proof. Consider the following Lyapunov function:

$$V_i(t) = y_i^T(t)y_i(t), i = 1, 2, \cdots, N.$$

For all $t \in \left[t_{k-1}^i, t_k^i\right)$, calculating the derivative of $V_i(t)$ along the system of (3.3) gives that

$$D^+V_i(t) = 2y_i^T(t)\left[\phi\left(t, y_i(t), y_i\left(t-\varrho(t)\right)\right) + \sum_{j=1}^{N} g_{ij}\Gamma y_j\left(t-\varsigma(t)\right)\right].$$

Based on Assumption 2.1, it can be obtained that

$$\begin{aligned} y_i^T(t)\phi\left(t, y_i(t), y_i\left(t-\varrho(t)\right)\right) &\leq \|y_i(t)\|\|\phi\left(t, y_i(t), y_i\left(t-\varrho(t)\right)\right)\| \\ &\leq \|y_i(t)\|\left(l_1\|y_i(t)\| + l_2\|y_i\left(t-\varrho(t)\right)\|\right) \\ &\leq \left(l_1 + \frac{1}{2}l_2\right)V_i(t) + \frac{l_2}{2}V_i\left(t-\varrho(t)\right). \end{aligned} \tag{3.4}$$

From the Cauchy inequality, one can obtain that

$$\begin{aligned} \sum_{j=1}^{N} g_{ij}y_i^T(t)\Gamma y_j\left(t-\varsigma(t)\right) =& g_{ii}y_i^T(t)\Gamma y_i\left(t-\varsigma(t)\right) + \sum_{j\neq i} g_{ij}y_i^T(t)\Gamma y_j\left(t-\varsigma(t)\right) \\ \leq& -\frac{g_{ii}}{2}\left[y_i^T(t)\Gamma^2 y_i(t) + y_i^T\left(t-\varsigma(t)\right)y_i\left(t-\varsigma(t)\right)\right] \\ &+ \sum_{j\neq i}\frac{g_{ij}}{2}\left[y_i^T(t)\Gamma^2 y_i(t) + y_j^T\left(t-\varsigma(t)\right)y_j\left(t-\varsigma(t)\right)\right] \\ =& -g_{ii}\gamma^2 V_i(t) - \frac{g_{ii}}{2}V_i\left(t-\varsigma(t)\right) + \sum_{j\neq i} g_{ij}V_j\left(t-\varsigma(t)\right). \end{aligned} \tag{3.5}$$

To sum up, it can be further deduced that

$$D^+V_i(t) \leq \left(2l_1 + l_2 - 2g_{ii}\gamma^2\right)V_i(t) + l_2V_i\left(t-\varrho(t)\right) - g_{ii}V_i\left(t-\varsigma(t)\right) + \sum_{j\neq i} g_{ij}V_j\left(t-\varsigma(t)\right). \tag{3.6}$$

When $t = t_k^i$, one has

$$V_i\left(t_k^{i+}\right) = (1+\mu)^2\, V_i\left(t_k^{i-}\right). \tag{3.7}$$

Case 1. *The whole impulse time sequence $\{t_k^i\}$ is only comprised of forced time, at which point Zeno behavior is clearly excluded by the definition of forced time.*

Case 2. *The whole impulse time sequence $\{t_k^i\}$ is only comprised of event-triggered time.*

Let

$$\Pi_i(t) = \begin{cases} V_i(t)\mathrm{e}^{\lambda(t-t_0)}, & t \in [t_0, +\infty), \\ V_i(t), & t \in [t_0 - d, t_0), \end{cases} \tag{3.8}$$

then the event-triggered mechanism (3.1) is equivalent to the following form:

$$\begin{aligned} &t_k^i = \min\left\{\sigma_k^i, \tau_k^i\right\}, \\ &\sigma_k^i = \inf\left\{t \geq t_{k-1}^i : \Pi_i(t) \geq a\mathrm{e}^{\lambda(t-t_{k-1}^i)}\Pi_i(t_{k-1}^i) + bV_{i0}\right\}. \end{aligned} \tag{3.9}$$

It should be noticed that

$$\Pi_i\left(t_{k-1}^i\right) \leq \mathrm{e}^{\lambda\left(t_k^i - t_{k-1}^i\right)}\Pi_i\left(t_{k-1}^i\right) + V_{i0} \leq \Pi_i\left(t_k^i\right).$$

Hence, there exists $s_k^i = \sup\left\{t \in \left[t_{k-1}^i, t_k^i\right) \,:\, \Pi_i(t) \leq \mathrm{e}^{\lambda\left(t_k^i - t_{k-1}^i\right)}\Pi_i\left(t_{k-1}^i\right) + V_{i0}\right\}$. Since $\Pi_i(t)$ is a continuous function, we have $\Pi_i\left(s_k^i\right) = \mathrm{e}^{\lambda\left(t_k^i - t_{k-1}^i\right)}\Pi_i\left(t_{k-1}^i\right) + V_{i0}$ and $\Pi_i(t) \geq \mathrm{e}^{\lambda\left(t_k^i - t_{k-1}^i\right)}\Pi_i\left(t_{k-1}^i\right) + V_{i0}$, for $t \in \left[s_k^i, t_k^i\right)$. Based on (3.7), the following inequality holds:

$$\begin{aligned}
\Pi_i\left(t_k^{i-}\right) &= a\mathrm{e}^{\lambda\left(t_k^i - t_{k-1}^i\right)}\Pi_i\left(t_{k-1}^i\right) + bV_{i0} \\
&\leq a\rho\mathrm{e}^{\lambda\left(t_k^i - t_{k-1}^i\right)}\Pi_i\left(t_{k-1}^{i-}\right) + bV_{i0} \\
&\leq a\rho\mathrm{e}^{\lambda\left(t_k^i - t_{k-2}^i\right)}\Pi_i\left(t_{k-2}^i\right) + bV_{i0}\left(1 + a\rho\mathrm{e}^{\lambda\left(t_k^i - t_{k-1}^i\right)}\right) \\
&\cdots\cdots \\
&\leq a\,(a\rho)^{k-1}\,\mathrm{e}^{\lambda\left(t_k^i - t_0\right)}V_{i0} + \sum_{l=0}^{k-1} bV_{i0}\,(a\rho)^l\,\mathrm{e}^{\lambda\left(t_k^i - t_{k-l}^i\right)} \\
&\leq \left(\mathrm{e}^{k(\lambda\eta + \ln a\rho) - \ln\rho} + \sum_{i=0}^{k-1} b\mathrm{e}^{i(\lambda\eta + \ln a\rho)}\right)V_{i0} \\
&\leq \left(\rho^{-1} + \frac{b}{1 - a\mathrm{e}^{\lambda\eta + \ln\rho}}\right)V_{i0},
\end{aligned} \tag{3.10}$$

where $\rho = (1+\mu)^2$. Thus, for $t \in \left[s_k^i, t_k^i\right)$, one can derive that

$$\begin{aligned}
\Pi_i\left(t - \varrho(t)\right) &\leq \begin{cases}
\Pi_i\left(t_k^{i-}\right), & t - \varrho(t) \in \left[t_{k-1}^i, t_k^i\right) \\
\Pi_i\left(t_{k-1}^{i-}\right), & t - \varrho(t) \in \left[t_{k-2}^i, t_{k-1}^i\right) \\
\vdots & \\
\Pi_i\left(t_1^{i-}\right), & t - \varrho(t) \in \left[t_0, t_1^i\right) \\
V_0, & t - \varrho(t) \in [t_0 - h, t_0)
\end{cases} \\
&\leq \frac{\rho^{-1} - a\mathrm{e}^{\lambda\eta} + b}{1 - \mathrm{e}^{\lambda\eta + \ln a\rho}}V_{i0} \\
&\leq \frac{\rho^{-1} - a\mathrm{e}^{\lambda\eta} + b}{1 - \mathrm{e}^{\lambda\eta + \ln a\rho}}\Pi_i(t).
\end{aligned} \tag{3.11}$$

Similarly,

$$\Pi_i\left(t - \varsigma(t)\right) \leq \frac{\rho^{-1} - a\mathrm{e}^{\lambda\eta} + b}{1 - \mathrm{e}^{\lambda\eta + \ln a\rho}}\Pi_i(t), \tag{3.12}$$

and

$$\Pi_j\left(t - \varsigma(t)\right) \leq \frac{\rho^{-1} - a\mathrm{e}^{\lambda\eta} + b}{1 - \mathrm{e}^{\lambda\eta + \ln a\rho}}V_{j0} = \frac{\rho^{-1} - a\mathrm{e}^{\lambda\eta} + b}{1 - \mathrm{e}^{\lambda\eta + \ln a\rho}}\frac{V_{j0}}{V_{i0}}V_{i0} \leq \frac{\rho^{-1} - a\mathrm{e}^{\lambda\eta} + b}{1 - \mathrm{e}^{\lambda\eta + \ln a\rho}}\frac{V_{j0}}{V_{i0}}\Pi_i(t).$$

Combined with the condition of theorem, it readily follows that

$$\begin{aligned} D^+\Pi_i(t) \leq & \left(2l_1 + l_2 - 2g_{ii}\gamma^2 + \lambda\right)\Pi_i(t) + l_2\mathrm{e}^{\lambda h}\Pi_i\left(t-\varrho(t)\right) - g_{ii}\mathrm{e}^{\lambda h}\Pi_i\left(t-\varsigma(t)\right) \\ & + \sum_{j\neq i} g_{ij}\mathrm{e}^{\lambda h}\Pi_j\left(t-\varsigma(t)\right) \\ \leq & \left(2l_1 + l_2 - 2g_{ii}\gamma^2 + \lambda + l_2\mathrm{e}^{\lambda h}\Theta - g_{ii}\mathrm{e}^{\lambda h}\Theta + \sum_{j\neq i} g_{ij}\mathrm{e}^{\lambda h}\frac{V_{j0}}{V_{i0}}\Theta\right)\Pi_i(t), \end{aligned} \tag{3.13}$$

where $\Theta = \frac{\rho^{-1} - a\mathrm{e}^{\lambda\eta} + b}{1-\mathrm{e}^{\lambda\eta+\ln a\rho}}$. By calculating the integration over the interval $t \in \left[s_k^i, t_k^i\right)$, one gets

$$\begin{aligned} \Pi_i\left(t_k^{i-}\right) \leq & \mathrm{e}^{\left[2l_1+l_2-2g_{ii}\gamma^2+\lambda+l_2\mathrm{e}^{\lambda h}\Theta-g_{ii}\mathrm{e}^{\lambda h}\Theta+\sum_{j\neq i} g_{ij}\mathrm{e}^{\lambda h}\frac{V_{j0}}{V_{i0}}\Theta\right]\left(t_k^i - s_k^i\right)}\Pi\left(s_k^i\right) \\ \leq & \mathrm{e}^{\left[2l_1+l_2-2g_{ii}\gamma^2+\lambda+l_2\mathrm{e}^{\lambda h}\Theta-g_{ii}\mathrm{e}^{\lambda h}\Theta+\sum_{j\neq i} g_{ij}\mathrm{e}^{\lambda h}\frac{V_{j0}}{V_{i0}}\Theta\right]\left(t_k^i - t_{k-1}^i\right)}\Pi\left(s_k^i\right). \end{aligned} \tag{3.14}$$

Therefore, $t_k^i - t_{k-1}^i \geq \frac{\ln(p\wedge q)}{2l_1+l_2-2g_{ii}\gamma^2+\lambda+l_2\mathrm{e}^{\lambda h}\Theta-g_{ii}\mathrm{e}^{\lambda h}\Theta+\sum_{j\neq i} g_{ij}\mathrm{e}^{\lambda h}\frac{V_{j0}}{V_{i0}}\Theta} > 0$, so that $t_k^i \to +\infty\,(k\to\infty)$ and $t_k \to +\infty\,(k\to\infty)$.

Case 3. *The whole impulse time sequence $\{t_k^i\}$ comprises the forced time and the event-triggered time together. It is clear from the foregoing discussion that the Zeno behavior is excluded.*

It means that there is no Zeno behavior. Next, we present the proof that the network (2.1) can achieve synchronization. From (3.1) and (3.7),

$$\begin{aligned} V_i(t) \leq & aV_i\left(t_{k-1}^i\right) + bV_{i0}\mathrm{e}^{-\lambda(t-t_0)} \\ \leq & a\rho V_i\left(t_{k-1}^{i-}\right) + bV_{i0}\mathrm{e}^{-\lambda(t-t_0)} \\ \leq & a\left(a\rho\right)V_i\left(t_{k-2}^i\right) + bV_{i0}\left(\mathrm{e}^{-\lambda(t-t_0)} + a\rho\mathrm{e}^{-\lambda\left(t_{k-1}^i - t_0\right)}\right) \\ \leq & \cdots \\ \leq & \left(a\left(a\rho\right)^{k-1} + b\mathrm{e}^{-\lambda(t-t_0)}\right)V_{i0} + \sum_{l=1}^{k-1} bV_{i0}\left(a\rho\right)^l\mathrm{e}^{-\lambda\left(t_{k-l}^i - t_0\right)} \\ \leq & \left[a\left(a\rho\right)^{k-1} + b\mathrm{e}^{-\lambda(t-t_0)} + b\left(k-1\right)\mathrm{e}^{-k\lambda\epsilon}\right]V_{i0} \\ \leq & \left[b\mathrm{e}^{-\lambda(t-t_0)} + \left(bk + \rho^{-1}\right)\mathrm{e}^{-k\lambda\epsilon}\right]V_{i0}. \end{aligned} \tag{3.15}$$

Hence, $\|y_i(t)\| \leq \sqrt{[b\mathrm{e}^{-\lambda(t-t_0)} + (bk+\rho^{-1})\,\mathrm{e}^{-k\lambda\epsilon}]V_{i0}}$, and $\lim\limits_{t\to+\infty}\|y_i(t)\| = 0$. The proof is completed. □

Remark 3.1. *The difficulty in applying event-triggered impulsive control to delayed systems is extracting delayed state information when avoiding Zeno behavior, and the related approach has been repeatedly investigated in [12]. However, this approach cannot be applied to a network directly, mainly because there is information exchange between network nodes, and this coupling effect further increases the difficulty of extracting delayed state information. In the proof of Theorem 3.1, we overcome this difficulty by attributing the terms in the Lyapunov function that contain coupling information to the initial values. However, this also makes our results relatively sensitive to the initial values and somewhat conservative.*

Remark 3.2. *Unlike conventional impulsive control based on the average dwell time method, e.g., [27–29], the time interval between impulses is not fixed; it depends on the divergence rate of the state vector. More specifically, when the error vector grows faster, it leads to quicker trigger control, and we have shown that a lower bound on the trigger interval for the same node does not lead to an infinite number of triggers in a finite time. Conversely, when the error grows more slowly, slower departure control can be allowed. This mechanism dictates that event-triggered impulse control will save more control resources than traditional impulsive control.*

3.2. Event-triggered pinning impulsive control strategy

As mentioned in the previous section, event-triggered impulsive control has the benefit of saving control resources compared with time-based impulsive control. On this basis, how to further reduce the consumption of control resources is the concern of this paper. Inspired by many works such as [30–32], this part will demonstrate that synchronization of the network can also be achieved by applying control to the partial node. Different from the previously proposed control strategy, these controlled nodes are controlled simultaneously at the impulse time t_k, and the impulse sequence $\{t_k\}$ is determined by the following event-triggered mechanism:

$$\begin{aligned} &t_k = \min\{\sigma_k, \tau_k\}, \\ &\sigma_k = \inf\left\{t \geq t_{k-1} : \sum_{i=1}^{N} y_i^T(t) y_i(t) \geq a \sum_{i=1}^{N} y_i^T(t_{k-1}) y_i(t_{k-1}) + bV_0 \mathrm{e}^{-\lambda(t-t_0)}\right\}, \end{aligned} \tag{3.16}$$

where $k \in \mathbb{Z}_+$, $a, b > 1$, $V_0 = \sup\limits_{s\in[-d,0]} \sum_{i=1}^{N} y_i^T(t_0+s) y_i(t_0+s)$, $y_i(t) = z_i(t) - s(t)$ is the error vector. In particular, τ_k represents the forced impulsive sequence, defined as $\tau_k = t_{k-1} + \eta$ with $\eta > 0$. The parameters a, b, and λ are core design parameters in the triggering condition, used to adjust the sensitivity of the triggering function to accommodate different system dynamics. The forced impulse parameters τ_k and η provide a safety backup to ensure system stability under worst-case scenarios. At the impulse time, the network is controlled by the following controller:

$$u_i(t) = \mu \sum_{k=1}^{\infty} y_i(t)\delta(t - t_k), i \in \mathcal{D}(t_k), \tag{3.17}$$

where $|1 + \mu| < 1$. Then the error systems can be rewritten as

$$\begin{cases} \dot{y}_i(t) = \phi(t, y_i(t), y_i(t - \varrho(t))) + \sum\limits_{j=1}^{N} g_{ij} \Gamma y_j(t - \varsigma(t)), t \neq t_k, \\ y_i(t_k^+) = (1 + \mu) y_i(t_k^-), i \in \mathcal{D}(t_k). \end{cases} \tag{3.18}$$

In the pinning event-triggered impulsive control strategy proposed in this part, the selection of pinned nodes is based on the following rule: At each event-triggered instant, the system detects the state error norm $\|y_i(t)\|$ of all nodes, where $y_i(t)$ denotes the state error of node i. The nodes are sorted according to the magnitude of their error norms, and the top l nodes with the largest error norms are selected as pinned nodes, forming the pinned node set $D(t) = \{p_1, p_2, \cdots, p_l\}$. The parameter l can be predetermined based on the network size and desired control performance, or adaptively adjusted according to practical requirements.

Remark 3.3. *The index $\mathcal{D}(t)$, which needs to be controlled impulsively, is defined as follows: At time instant t, one can reorder the vectors of error states $y_1(t), y_2(t), \cdots, y_N(t)$, as $\|y_{p_1}(t)\| \geq \|y_{p_2}(t)\| \geq \cdots \geq \|y_{p_N}(t)\|$, then $\mathcal{D}(t) = \{p_1, p_2, \cdots, p_l\}$. If there is more than one state with the same norm, any node that has the same norm can be chosen. Once the impulse time is determined, the centralized impulsive controller selects the nodes to be controlled and sends control signals to them.*

Theorem 3.2. *Let $\rho = \frac{N+l\mu(\mu+2)}{N} \in (0,1)$ and suppose that Assumption 2.1 holds. If there exist constants $a, b > 1$, η, $\lambda > 0$ satisfying $\lambda\eta + \ln(a\rho) < 0$, then the complex networks (2.1) with event-triggered mechanism (3.16) and controller (3.17) is globally synchronized to $s(t)$. Moreover, there is no Zeno behavior, and the inter-execution times $\{t_k - t_{k-1}\}_{k\in\mathbb{Z}_+}$ have a lower bound:*

$$\epsilon = \min\left\{\frac{\ln(a \wedge b)}{2l_1 + l_2 + \gamma + \lambda + \frac{\left(l_2+\gamma\lambda_{\max}\left(G^TG\right)\right)\left(\rho^{-1}-ae^{\lambda\eta}+b\right)}{1-e^{\lambda\eta+\ln a\rho}}e^{\lambda h}}, \eta\right\}. \tag{3.19}$$

Proof. Consider the following Lyapunov function:

$$V(t) = \sum_{i=1}^{N} y_i^T(t) y_i(t).$$

For all $t \in [t_{k-1}, t_k)$, calculating the derivative of $V_i(t)$ along the system of (3.18) gives that

$$D^+V(t) = 2\sum_{i=1}^{N} y_i^T(t)\left[\phi\left(t, y_i(t), y_i\left(t-\tau(t)\right)\right) + \sum_{j=1}^{N} g_{ij}\Gamma y_j\left(t-\varsigma(t)\right)\right].$$

Based on Assumption 2.1, it can be obtained that

$$\begin{aligned}\sum_{i=1}^{N} y_i^T(t)\phi\left(t, y_i(t), y_i\left(t-\varrho(t)\right)\right) &\leq \sum_{i=1}^{N} \|y_i(t)\|\|\phi\left(t, y_i(t), y_i\left(t-\varrho(t)\right)\right)\| \\ &\leq \sum_{i=1}^{N} \|y_i(t)\|\left(l_1\|y_i(t)\| + l_2\|y_i\left(t-\varrho(t)\right)\|\right) \\ &\leq \left(l_1 + \frac{1}{2}l_2\right)V(t) + \frac{l_2}{2}V\left(t-\varrho(t)\right).\end{aligned} \tag{3.20}$$

From the Cauchy inequality, one can get

$$\begin{aligned}\sum_{i=1}^{N}\sum_{j=1}^{N} g_{ij}y_i^T(t)\Gamma y_j\left(t-\varsigma(t)\right) &= \sum_{i=1}^{N}\sum_{j=1}^{N} g_{ij}\sum_{k=1}^{n}\gamma_k y_{ik}(t)y_{jk}\left(t-\varsigma(t)\right) \\ &= \sum_{k=1}^{n}\gamma_k y^k(t)G\left(y^k\left(t-\varsigma(t)\right)\right)^T \\ &\leq \frac{1}{2}\sum_{k=1}^{n}\gamma_k\left[y^k\left(t-\varsigma(t)\right)G^TG\left(y^k\left(t-\varsigma(t)\right)\right)^T + y^k(t)\left(y^k(t)\right)^T\right] \\ &\leq \frac{\gamma\lambda_{\max}\left(G^TG\right)}{2}V\left(t-\varsigma(t)\right) + \frac{\gamma}{2}V(t),\end{aligned} \tag{3.21}$$

where $\gamma = \max\{\gamma_1, \gamma_2, \cdots, \gamma_n\}$, $y^k(t) = (y_{1k}, y_{2k}, \cdots, y_{Nk})$. From (3.20) and (3.21),

$$D^+V(t) \leq (2l_1 + l_2 + \gamma)\, V(t) + l_2 V\left(t - \varrho(t)\right) + \gamma\lambda_{\max}\left(G^T G\right) V\left(t - \varsigma(t)\right). \tag{3.22}$$

When $t = t_k$, one has

$$\begin{aligned} V\left(t_k^+\right) &= \sum_{i=1}^{N} y_i^T\left(t_k^+\right) y_i\left(t_k^+\right) \\ &= \sum_{i\in\mathcal{D}} (1+\mu)^2\, y_i^T\left(t_k^-\right) y_i\left(t_k^-\right) + \sum_{i\notin\mathcal{D}} y_i^T\left(t_k^-\right) y_i\left(t_k^-\right) \\ &\leq \sum_{i\in\mathcal{D}} (1+\mu)^2\, y_i^T\left(t_k^-\right) y_i\left(t_k^-\right) + (N-l)\|y_{p_{l+1}}(t)\|^2 \\ &= \sum_{i\in\mathcal{D}} (1+\mu)^2\, y_i^T\left(t_k^-\right) y_i\left(t_k^-\right) + \frac{N-l}{l} l\|y_{p_{l+1}}(t)\|^2 \\ &\leq \left[(1+\mu)^2 + \frac{N-l}{l}\right] \sum_{i\in\mathcal{D}} y_i^T\left(t_k^-\right) y_i\left(t_k^-\right). \end{aligned} \tag{3.23}$$

On the other hand,

$$\rho V\left(t_k^-\right) \leq \rho \frac{N}{l} \sum_{i\in\mathcal{D}} y_i^T\left(t_k^-\right) y_i\left(t_k^-\right). \tag{3.24}$$

According to (3.23) and (3.24), it can be further obtained that

$$V\left(t_k^+\right) \leq \rho V\left(t_k^-\right). \tag{3.25}$$

Case 1. *The whole impulse time sequence $\{t_k\}$ is only comprised of forced time, at which point Zeno behavior is clearly ruled out by the definition of forced time.*

Case 2. *The whole impulse time sequence $\{t_k\}$ is only comprised of triggering times.*

Let

$$\Pi(t) = \begin{cases} V(t)\mathrm{e}^{\lambda(t-t_0)}, & t \in [t_0, +\infty), \\ V(t), & t \in [t_0 - h, t_0), \end{cases} \tag{3.26}$$

then the event-triggered mechanism (3.16) is equivalent to the following form:

$$\begin{aligned} t_k &= \min\left\{t_k^*, \tau_k\right\}, \\ t_k^* &= \inf\left\{t \geq t_{k-1} : \Pi(t) \geq a\mathrm{e}^{\lambda(t-t_{k-1})} V(t_{k-1}) + bV_0\right\}. \end{aligned} \tag{3.27}$$

It should be noticed that

$$\Pi\left(t_{k-1}\right) \leq \mathrm{e}^{\lambda(t_k - t_{k-1})}\Pi\left(t_{k-1}\right) + V_0 \leq \Pi\left(t_k\right).$$

Hence, there exists $s_k = \sup\left\{t \in [t_{k-1}, t_k) \ : \ \Pi(t) \leq \mathrm{e}^{\lambda(t_k - t_{k-1})}\Pi\left(t_{k-1}\right) + V_0\right\}$. Since $\Pi(t)$ is a continuous function, we have $\Pi\left(s_k\right) = \mathrm{e}^{\lambda(t_k - t_{k-1})}\Pi\left(t_{k-1}\right) + V_0$ and $\Pi(t) \geq \mathrm{e}^{\lambda(t_k - t_{k-1})}\Pi\left(t_{k-1}\right) + V_0$, for $t \in [s_k, t_k)$. Based

on (3.25), the following inequality holds:

$$\begin{aligned}\Pi\left(t_k^-\right) &= a\mathrm{e}^{\lambda(t_k-t_{k-1})}\Pi\left(t_{k-1}\right)+bV_0\\ &\le a\rho\mathrm{e}^{\lambda(t_k-t_{k-1})}\Pi\left(t_{k-1}^-\right)+bV_0\\ &\le a\rho\mathrm{e}^{\lambda(t_k-t_{k-2})}\Pi\left(t_{k-2}\right)+bV_0\left(1+a\rho\mathrm{e}^{\lambda(t_k-t_{k-1})}\right)\\ &\cdots\cdots\\ &\le a\left(a\rho\right)^{k-1}\mathrm{e}^{\lambda(t_k-t_0)}V_0+\sum_{i=0}^{k-1}bV_0\left(a\rho\right)^i\mathrm{e}^{\lambda(t_k-t_{k-i})}\\ &\le\left(\mathrm{e}^{k(\lambda\eta+\ln a\rho)-\ln\rho}+\sum_{i=0}^{k-1}b\mathrm{e}^{i(\lambda\eta+\ln a\rho)}\right)V_0\\ &\le\left(\rho^{-1}+\frac{b}{1-a\mathrm{e}^{\lambda\eta+\ln\rho}}\right)V_0.\end{aligned}\tag{3.28}$$

Thus, for $t\in[s_k,t_k)$, we can derive that

$$\begin{aligned}\Pi\left(t-\varrho(t)\right)\le&\begin{cases}\Pi\left(t_k^-\right), & t-\varrho(t)\in[t_{k-1},t_k)\\ \Pi\left(t_{k-1}^-\right), & t-\varrho(t)\in[t_{k-2},t_{k-1})\\ \vdots & \\ \Pi\left(t_1^-\right), & t-\varrho(t)\in[t_0,t_1)\\ V_0, & t-\varrho(t)\in[t_0-h,t_0)\end{cases}\\ \le&\frac{\rho^{-1}-a\mathrm{e}^{\lambda\eta}+b}{1-\mathrm{e}^{\lambda\eta+\ln a\rho}}V_0\\ \le&\frac{\rho^{-1}-a\mathrm{e}^{\lambda\eta}+b}{1-\mathrm{e}^{\lambda\eta+\ln a\rho}}\Pi(t).\end{aligned}\tag{3.29}$$

Similarly,

$$\Pi\left(t-\varsigma(t)\right)\le\frac{\rho^{-1}-a\mathrm{e}^{\lambda\eta}+b}{1-\mathrm{e}^{\lambda\eta+\ln a\rho}}\Pi(t).\tag{3.30}$$

Combining (3.22), (3.26), (3.29), and (3.30), it follows that

$$D^+\Pi(t)\le\left[2l_1+l_2+\gamma+\lambda+\frac{\left(l_2+\gamma\lambda_{\max}\left(G^TG\right)\right)\left(\rho^{-1}-a\mathrm{e}^{\lambda\eta}+b\right)}{1-\mathrm{e}^{\lambda\eta+\ln a\rho}}\mathrm{e}^{\lambda h}\right]\Pi(t).$$

By calculating the integration over the interval $t\in[s_k,t_k)$, one obtains

$$\begin{aligned}\Pi\left(t_k^-\right)\le&\mathrm{e}^{\left[2l_1+l_2+\gamma+\lambda+\frac{\left(l_2+\gamma\lambda_{\max}\left(G^TG\right)\right)\left(\rho^{-1}-a\mathrm{e}^{\lambda\eta}+b\right)}{1-\mathrm{e}^{\lambda\eta+\ln a\rho}}\mathrm{e}^{\lambda h}\right](t_k-s_k)}\Pi\left(s_k\right)\\ \le&\mathrm{e}^{\left[2l_1+l_2+\gamma+\lambda+\frac{\left(l_2+\gamma\lambda_{\max}\left(G^TG\right)\right)\left(\rho^{-1}-a\mathrm{e}^{\lambda\eta}+b\right)}{1-\mathrm{e}^{\lambda\eta+\ln a\rho}}\mathrm{e}^{\lambda h}\right](t_k-t_{k-1})}\Pi\left(s_k\right).\end{aligned}\tag{3.31}$$

Therefore, $t_k-t_{k-1}\ge\frac{\ln(a\wedge b)}{2l_1+l_2+\gamma+\lambda+\frac{\left(l_2+\gamma\lambda_{\max}\left(G^TG\right)\right)\left(\rho^{-1}-a\mathrm{e}^{\lambda\eta}+b\right)}{1-\mathrm{e}^{\lambda\eta+\ln a\rho}}\mathrm{e}^{\lambda h}}$.

Case 3. *The whole impulse time sequence $\{t_k\}$ comprises the forced time and the event-triggered time together. It is clear from the foregoing discussion that Zeno behavior is excluded.*

It means that there is no Zeno behavior. Next, we will prove that the network can achieve synchronization. From (3.16) and (3.25), we can get

$$\begin{aligned} V(t) &\leq aV\left(t_{k-1}\right) + bV_0 \mathrm{e}^{-\lambda(t-t_0)} \\ &\leq a\rho V\left(t_{k-1}^{-}\right) + bV_0 \mathrm{e}^{-\lambda(t-t_0)} \\ &\leq a\left(a\rho\right) V\left(t_{k-2}\right) + bV_0\left(\mathrm{e}^{-\lambda(t-t_0)} + a\rho \mathrm{e}^{-\lambda\left(t_{k-1}-t_0\right)}\right) \\ &\cdots \\ &\leq \left(a\left(a\rho\right)^{k-1} + b\mathrm{e}^{-\lambda(t-t_0)}\right) V_0 + \sum_{i=1}^{k-1} bV_0\left(a\rho\right)^i \mathrm{e}^{-\lambda\left(t_{k-i}-t_0\right)} \\ &\leq \left[a\left(a\rho\right)^{k-1} + b\mathrm{e}^{-\lambda(t-t_0)} + b\left(k-1\right)\mathrm{e}^{-k\lambda\epsilon}\right] V_0 \\ &\leq \left[b\mathrm{e}^{-\lambda(t-t_0)} + \left(bk + \rho^{-1}\right)\mathrm{e}^{-k\lambda\epsilon}\right] V_0. \end{aligned} \tag{3.32}$$

Hence, $\|e(t)\| \leq \sqrt{[b\mathrm{e}^{-\lambda(t-t_0)} + (bk+\rho^{-1})\,\mathrm{e}^{-k\lambda\epsilon}]V_0}$. The proof is completed. □

Remark 3.4. *During the application of impulsive control, it is important to construct a relationship between the divergence rate of the system and the impulse parameters, such as the condition (6) in [33]. While the topology of the network and the continuous dynamics of the nodes both affect only the divergence rate, in order to synchronize the network, it is necessary to select a suitable average impulse interval to satisfy the above conditions. In event-triggered impulsive control, the impulse interval is determined by the event-triggered mechanism, so the information about the topology of the network and the continuous dynamics of the nodes is embedded in the lower bound (3.19) of the impulse interval rather than in the condition.*

4. Numerical simulation

In this section, we present two numerical examples to validate the theoretical results derived in the previous sections. The system under consideration consists of an array of 20 linearly coupled nodes, each governed by the following equations:

$$\begin{aligned} \dot{s}(t) &= \tilde{\phi}\left(t, s(t), s\left(t-\varrho(t)\right)\right) = Bs(t) + Cf\left(s(t)\right) + Df\left(s\left(t-\varrho(t)\right)\right), \\ \dot{z}_i\left(t\right) &= Bz_i(t) + Cf\left(z_i(t)\right) + Df\left(z_i\left(t-\varrho(t)\right)\right) + \sum_{j=1}^{N} g_{ij}\Gamma z_j\left(t-\varsigma\left(t\right)\right) + u_i\left(t\right), i = 1, 2, \cdots, 20, \end{aligned}$$

where $B = \begin{bmatrix} -1 & 0 \\ 0 & -1 \end{bmatrix}$, $C = \begin{bmatrix} 1+\frac{\pi}{4} & 20 \\ 0.1 & 1+\frac{\pi}{4} \end{bmatrix}$, $D = \begin{bmatrix} -\frac{13\sqrt{2}\pi}{40} & 0.1 \\ 0.1 & -\frac{13\sqrt{2}\pi}{40} \end{bmatrix}$, $\Gamma = \begin{bmatrix} 1 & 0 \\ 0 & 1 \end{bmatrix}$, $f\left(s(t)\right) = \left[\frac{1}{2}(|s_1(t)+1| - |s_1(t)-1|), \quad \frac{1}{2}(|s_2(t)+1| - |s_2(t)-1|)\right]^T$, $\varrho(t) = \frac{\mathrm{e}^t}{10(\mathrm{e}^t+1)}$, and $\varsigma\left(t\right) = \frac{1}{10(\mathrm{e}^t+1)}$. The

coupling matrix G between network nodes is given as follows:

$$G = \begin{pmatrix}
-1 & 1 & 0 & 0 & 0 & 0 & 0 & 0 & 0 & 0 & 0 & 0 & 0 & 0 & 0 & 0 & 0 & 0 & 0 & 0 \\
0 & -1 & 1 & 0 & 0 & 0 & 0 & 0 & 0 & 0 & 0 & 0 & 0 & 0 & 0 & 0 & 0 & 0 & 0 & 0 \\
0 & 0 & -1 & 1 & 0 & 0 & 0 & 0 & 0 & 0 & 0 & 0 & 0 & 0 & 0 & 0 & 0 & 0 & 0 & 0 \\
0 & 0 & 0 & -1 & 1 & 0 & 0 & 0 & 0 & 0 & 0 & 0 & 0 & 0 & 0 & 0 & 0 & 0 & 0 & 0 \\
0 & 0 & 0 & 0 & -1 & 1 & 0 & 0 & 0 & 0 & 0 & 0 & 0 & 0 & 0 & 0 & 0 & 0 & 0 & 0 \\
0 & 0 & 0 & 0 & 0 & -1 & 1 & 0 & 0 & 0 & 0 & 0 & 0 & 0 & 0 & 0 & 0 & 0 & 0 & 0 \\
0 & 0 & 0 & 0 & 0 & 0 & -1 & 1 & 0 & 0 & 0 & 0 & 0 & 0 & 0 & 0 & 0 & 0 & 0 & 0 \\
0 & 0 & 0 & 0 & 0 & 0 & 0 & -1 & 1 & 0 & 0 & 0 & 0 & 0 & 0 & 0 & 0 & 0 & 0 & 0 \\
0 & 0 & 0 & 0 & 0 & 0 & 0 & 0 & -1 & 1 & 0 & 0 & 0 & 0 & 0 & 0 & 0 & 0 & 0 & 0 \\
0 & 0 & 0 & 0 & 0 & 0 & 0 & 0 & 0 & -1 & 1 & 0 & 0 & 0 & 0 & 0 & 0 & 0 & 0 & 0 \\
0 & 0 & 0 & 0 & 0 & 0 & 0 & 0 & 0 & 0 & -1 & 1 & 0 & 0 & 0 & 0 & 0 & 0 & 0 & 0 \\
0 & 0 & 0 & 0 & 0 & 0 & 0 & 0 & 0 & 0 & 0 & -1 & 1 & 0 & 0 & 0 & 0 & 0 & 0 & 0 \\
0 & 0 & 0 & 0 & 0 & 0 & 0 & 0 & 0 & 0 & 0 & 0 & -1 & 1 & 0 & 0 & 0 & 0 & 0 & 0 \\
0 & 0 & 0 & 0 & 0 & 0 & 0 & 0 & 0 & 0 & 0 & 0 & 0 & -1 & 1 & 0 & 0 & 0 & 0 & 0 \\
0 & 0 & 0 & 0 & 0 & 0 & 0 & 0 & 0 & 0 & 0 & 0 & 0 & 0 & -1 & 1 & 0 & 0 & 0 & 0 \\
0 & 0 & 0 & 0 & 0 & 0 & 0 & 0 & 0 & 0 & 0 & 0 & 0 & 0 & 0 & -1 & 1 & 0 & 0 & 0 \\
0 & 0 & 0 & 0 & 0 & 0 & 0 & 0 & 0 & 0 & 0 & 0 & 0 & 0 & 0 & 0 & -1 & 1 & 0 & 0 \\
0 & 0 & 0 & 0 & 0 & 0 & 0 & 0 & 0 & 0 & 0 & 0 & 0 & 0 & 0 & 0 & 0 & -1 & 1 & 0 \\
0 & 0 & 0 & 0 & 0 & 0 & 0 & 0 & 0 & 0 & 0 & 0 & 0 & 0 & 0 & 0 & 0 & 0 & -1 & 1 \\
1 & 0 & 0 & 0 & 0 & 0 & 0 & 0 & 0 & 0 & 0 & 0 & 0 & 0 & 0 & 0 & 0 & 0 & 0 & -1
\end{pmatrix}.$$

Define $e_{ij}(t) = z_{ij}(t) - s_j(t)(i = 1, 2, \cdots, 20, j = 1, 2)$. As shown in Figure 1, when the complex dynamical networks are uncontrolled, only the second component of the error vector can be controlled to a small extent, and the error of the first component remains large.

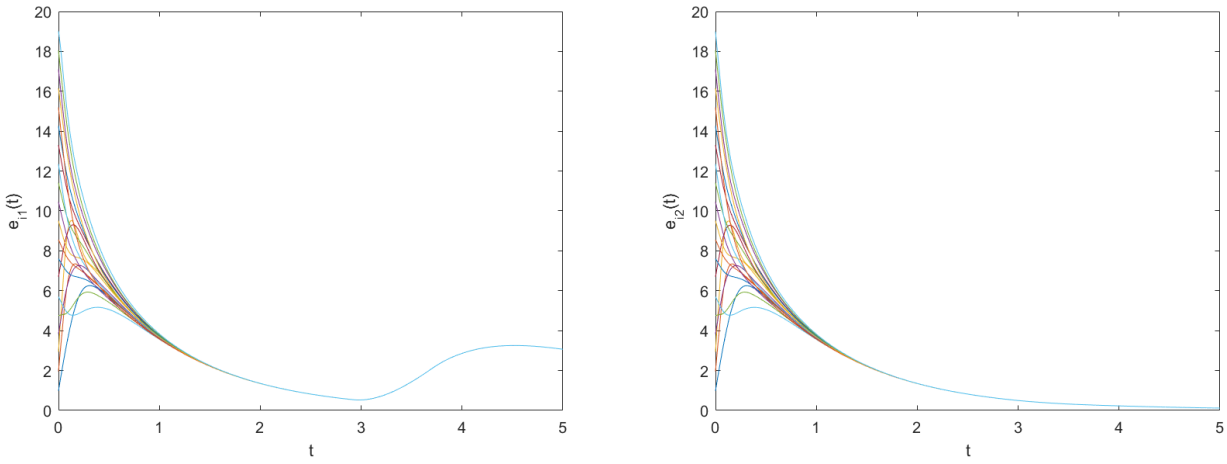

Figure 1. The state error without controller.

Example 4.1. *For the event-triggered mechanism and impulsive controller design, we select the impulsive gain parameter as* $\mu = -1.5$. *This choice yields* $(1 + \mu)^2 = 0.25$, *ensuring the contraction property of the impulsive control law. Further, we set the triggering parameters as* $\lambda = 1.5$ *(the*

convergence rate), $\eta = 0.01$ *(the triggering threshold), and the bounding constants* $a = 1.1$, $b = 2.5$ *to satisfy the stability conditions. A straightforward calculation demonstrates that the selected parameters satisfy the key stability criterion in Theorem 3.1:*

$$\lambda\eta + \ln\left[a(1+\mu)^2\right] \approx 1.5 \times 0.01 + \ln[1.1 \times 0.25] < -1.27 < 0.$$

This inequality guarantees the exponential convergence of the error dynamics under the proposed control scheme.

As illustrated in Figure 2, both components of the error vector are effectively regulated and maintained within a small neighborhood of zero under the action of the designed impulsive controller. The first component (typically representing positional error) and the second component (often corresponding to velocity or derivative error) exhibit uniform boundedness, confirming the theoretical predictions of Theorem 3.1. This numerical result underscores the efficacy of the proposed control strategy in achieving system stabilization through event-triggered impulsive actions.

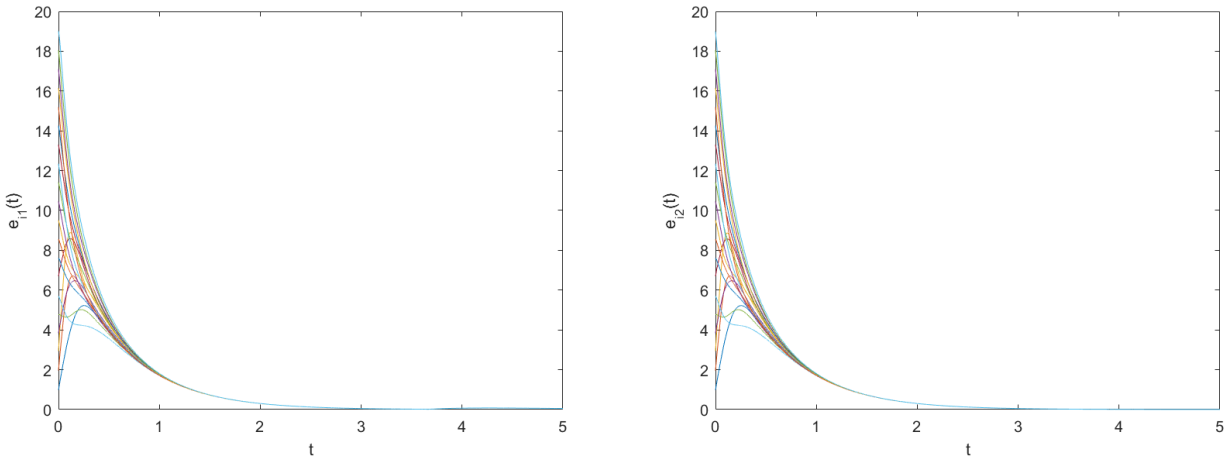

Figure 2. The state error with controller (3.2).

To more clearly depict the dynamic behavior at event-triggered impulsive instants, we have added special markings for the triggering instants in Figure 3. For ease of presentation, we have aggregated the triggering events of all nodes onto a single line. It should be noted that we present the triggering events of all nodes on the same line primarily to highlight the temporal characteristics of the triggering instants rather than the distribution across different nodes. In the proposed pinning control strategy, the event-triggering condition depends on the synchronization error of the entire network, making the triggering instants of individual nodes highly correlated. If the triggering instants of each node were plotted on separate horizontal lines, while this would distinguish the triggering behavior of different nodes, it would make the figure cluttered and difficult to intuitively capture the overall temporal distribution of triggering events. In contrast, aggregating the triggering events of all nodes onto a single line allows for a clearer presentation of the time series characteristics of the triggering instants, facilitating the observation of the trend in inter-event intervals and the regulatory effect of the dynamic event-triggered mechanism on the triggering frequency. This aggregated presentation aligns with the analytical focus of this paper, which emphasizes triggering timing and the number of triggers.

Specifically, we use blue dots to precisely mark the occurrence of each event-triggered impulsive instant, where each dot represents one triggering event. This dot-plot format clearly reflects the distribution characteristics of the triggering instants and the regulatory effect of the dynamic event-triggering mechanism on the triggering frequency. Through the above graphical processing, the instantaneous jump characteristics of event-triggered impulsive control and the temporal relationship of triggering are intuitively presented.

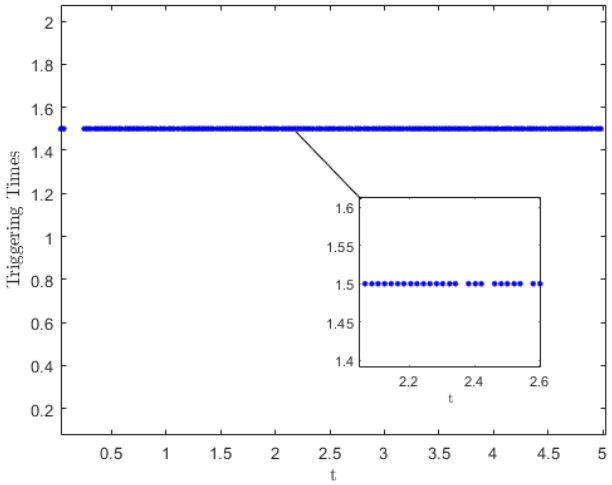

Figure 3. Triggering times.

Example 4.2. *In this numerical experiment, we investigate the effectiveness of the proposed impulsive control strategy when applied to a partially controlled network, where only 15 out of all nodes are subject to control inputs. In this part, the network consists of 20 nodes in total, among which 15 nodes are selected for pinning control. The selection of pinned nodes adopts a dynamic strategy based on error norms: At each impulsive instant, the system detects the state error norms of all nodes and selects the top 15 nodes with the largest error norms as pinned nodes. This selection method dynamically adjusts the pinned nodes according to the real-time system state, prioritizing control on nodes that deviate most severely from the desired trajectory, thereby effectively improving control efficiency. The impulsive gain is set to* $\mu = -1.5$*, resulting in a contraction factor* $\rho = \frac{(1+\mu)^2 l+(N-l)}{N} = 0.4375$*. The remaining parameters* $\lambda = 1.5$ *(convergence rate),* $\eta = 0.01$ *(event-triggering threshold), and bounding constants* $a = 1.1$*,* $b = 2.5$*–are kept consistent with Example 4.1 to ensure a fair comparison.*

The selected parameters satisfy the key stability criterion in Theorem 3.2, as confirmed by the following calculation:

$$\lambda\eta + \ln(a\rho) = 1.5 \times 0.01 + \ln(1.1 \times 0.4375) \approx -0.71 < 0.$$

This inequality ensures that the error dynamics under partial control remain exponentially stable, albeit with a modified convergence rate compared to the fully controlled case. The simulation results, depicted in Figure 4, demonstrate two key observations:

1) Error suppression: Both components of the error vector (typically representing positional and derivative errors) are confined to a significantly smaller range compared to the uncontrolled case (Figure 1), validating the controller's efficacy even with partial node actuation.

2) Convergence rate trade-off: In contrast to the fully controlled scenario (Figure 2), the error convergence to zero is slower under partial control, reflecting the inherent trade-off between control effort and system performance. These findings robustly support the theoretical claims of Theorem 3.2, confirming that the proposed control strategy remains effective under partial network actuation, albeit with a moderated convergence speed.

To verify the effectiveness of the proposed pinning dynamic event-triggered impulsive control strategy in reducing the triggering frequency, we conducted a comparative simulation between this strategy and the general event-triggered impulsive control strategy. As shown in Figure 5, during the simulation period from 0 to 5 seconds, the proposed pinning dynamic event-triggered impulsive control strategy triggered a total of 44 times, while the general event-triggered impulsive control strategy triggered 61 times. The comparison results show that, under the premise of ensuring system synchronization performance, the proposed strategy reduces the number of triggers by approximately 27.9 % compared with the conventional method, effectively lowering the communication burden and control update frequency. This demonstrates the superiority of the dynamic event-triggering mechanism in impulsive control.

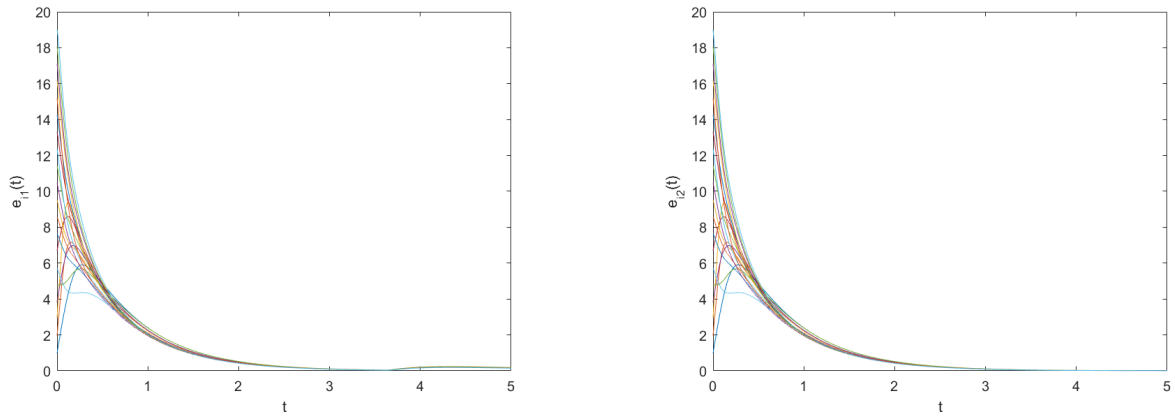

Figure 4. The state error with controller (3.17).

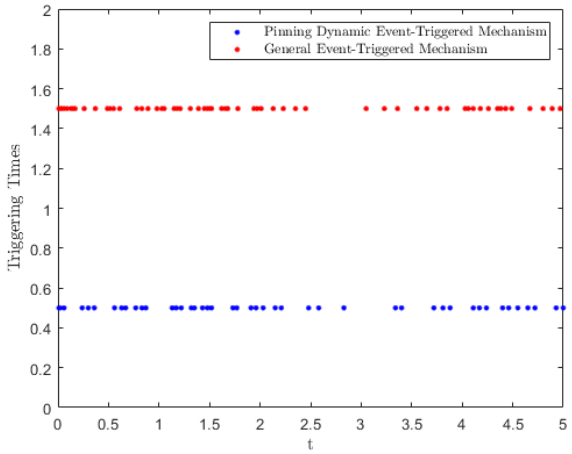

Figure 5. Triggering times.

5. Conclusions

In this paper, a class of delayed networks with the event-triggered impulsive control problem is investigated, for which a distributed event-triggered impulsive control strategy and an event-triggered pinning impulsive control strategy are designed to ensure the synchronization of the network. In addition, numerical simulation examples demonstrate the validity of the proposed theory. However, it should be noted that this work does not address the distributed event-triggered pinning impulsive control strategy, in which each node independently implements an event-triggered mechanism while impulsive control is applied only to a subset of nodes in the network. This strategy combines distributed triggering rules with pinning impulsive control, leading the system to evolve into a complex impulsive system with multiple asynchronous jump instants. In the Lyapunov stability analysis, the coupling between the independently generated triggering instants of multiple nodes and the selection of pinned nodes introduces significant challenges, substantially increasing the analytical difficulty. This more challenging scenario will be a key focus of our future work.

Author contributions

Jiayi Cai: Conceptualization, methodology, project administration, and writing-original draft; Jiang Yu: Software, writing-review & editing; Ze You: Formal analysis, project administration, and writing-review & editing; Chenglin Jing: Supervision, project administration, and final review and editing. All authors have read and approved the final version of the manuscript for publication.

Use of Generative-AI tools declaration

The authors declare that they have not used Artificial Intelligence (AI) tools in the creation of this article.

Acknowledgments

This research was supported by the National Natural Science Foundation of China under grants 62403157, 12461030; in part by the Guizhou Provincial Basic Research Program (Natural Science) under grants Qiankehejichu MS [2025] 233 and Qiankehejichu MS [2025] 234; in part by the Young Scientist Initiative Basic Research Program of Guizhou Province under grants QianKeHeJiChu-[2024] Youth 186 and QianKeHeJiChu [2025] QN. 361, and in part by the project of Young Scientific and Technical Talents Development of Education Department of Guizhou Province under grant [2024] No. 82.

Conflict of interest

The authors affirm that they have no conflict of interest.

References

1. J. Xiao, Y. Li, Deep analysis on MLSY for fractional-order higher-dimension-valued neural networks under the action of free quadratic coefficients, *Expert Syst. Appl.*, **298** (2026), 129586. https://doi.org/10.1016/j.eswa.2025.129586
2. R. Luo, J. Ren, K. Shi, Stability analysis of delayed T-S fuzzy power system via a cubic function negative determination lemma, *Nonlinear Dyn.*, **113** (2025), 5439–5456. https://doi.org/10.1007/s11071-024-10505-1
3. C. Yi, J. Cai, R. Guo, Synchronization of a class of nonlinear multiple neural networks with delays via a dynamic event-triggered impulsive control strategy, *Electron. Res. Arch.*, **32** (2024), 4581–4603. https://doi.org/10.3934/era.2024208
4. H. Fan, K. Shi, Z. Guo, A. Zhou, J. Cai, Finite-time synchronization and Mittag–Leffler synchronization for uncertain fractional-order delayed cellular neural networks with fuzzy operators via nonlinear adaptive control, *Fractal Fract.*, **9** (2025), 634. https://doi.org/10.3390/fractalfract9100634
5. X. Ruan, Z. Du, Z. Tang, J. Feng, J. Wang, Bipartite consensus for multi-agent systems under distributed sequential scaling attacks: An edge-based event-triggered scheme, *Appl. Math. Comput.*, **523** (2026), 130025. https://doi.org/10.1016/j.amc.2026.130025
6. L. Zhang, J. Lu, B. Jiang, C. Huang, Distributed synchronization of delayed dynamic networks under asynchronous delay-dependent impulsive control, *Chaos Solitons Fract.*, **168** (2023), 113121. https://doi.org/10.1016/j.chaos.2023.113121
7. H. Fan, H. Wen, K. Shi, J. Xiao, New fixed-time synchronization criteria for fractional-order fuzzy cellular neural networks with bounded uncertainties and transmission delays via multi-module control schemes, *Fractal Fract.*, **10** (2026), 91. https://doi.org/10.3390/fractalfract10020091
8. J. Suo, H. Hu, L. Xu, Delay-dependent impulsive control for lag quasi-synchronization of stochastic complex dynamical networks, *Math. Comput. Simulation*, **211** (2023), 134–153. https://doi.org/10.1016/j.matcom.2023.04.004
9. J. Cai, C. Yi, X. Luo, C. Xiao, Output feedback tracking consensus of switched stochastic uncertain multi-agent systems via event-triggered control, *IEEE Syst. J.*, **19** (2025), 130–141. https://doi.org/10.1109/JSYST.2024.3511914
10. Y. Lin, A. Lindquist, Synchronization of nonlinear delayed semi-Markov jump neural networks via distributed delayed impulsive control, *Systems Control Lett.*, **174** (2023), 105489. https://doi.org/10.1016/j.sysconle.2023.105489
11. X. Li, T. Zhang, J. Wu, Input-to-state stability of impulsive systems via event-triggered impulsive control, *IEEE Trans. Cybern.*, **52** (2022), 7187–7195. https://doi.org/10.1109/TCYB.2020.3044003
12. X. Li, X. Yang, J. Cao, Event-triggered impulsive control for nonlinear delay systems, *Automatica*, **117** (2020), 108981. https://doi.org/10.1016/j.automatica.2020.108981
13. M. Wang, X. Li, P. Duan, Event-triggered delayed impulsive control for nonlinear systems with application to complex neural networks, *Neural Netw.*, **150** (2022), 213–221. https://doi.org/10.1016/j.neunet.2022.03.007

14. J. Li, Q. Zhu, Event-triggered impulsive control of stochastic functional differential systems, *Chaos Solitons Fract.*, **170** (2023), 113416. https://doi.org/10.1016/j.chaos.2023.113416

15. J. Chen, B. Chen, Z. Zeng, Synchronization in multiple neural networks with delay and disconnected switching topology via event-triggered impulsive control strategy, *IEEE Trans. Ind. Electron.*, **68** (2021), 2491–2500. https://doi.org/10.1109/TIE.2020.2975498

16. D. Peng, X. Li, Leader-following synchronization of complex dynamic networks via event-triggered impulsive control, *Neurocomputing*, **412** (2020), 1–10. https://doi.org/10.1016/j.neucom.2020.05.071

17. H. Wang, Consensus of first-order multi-agent systems via event-triggered impulsive control, In: *2021 China automation congress (CAC)*, Beijing: IEEE, 2021, 3920–3925. https://doi.org/10.1109/CAC53003.2021.9727406

18. J. Ni, J. Liu, Q. Yang, H. Dai, Consensus of second-order multi-agent systems via event-triggered impulsive control, In: *2017 Chinese automation congress (CAC)*, Jinan: IEEE, 2017, 4346–4350. https://doi.org/10.1109/CAC.2017.8243544

19. W. H. Chen, W. X. Zheng, X. Lu, Impulsive stabilization of a class of singular systems with time-delays, *Automatica*, **83** (2017), 28–36. https://doi.org/10.1016/j.automatica.2017.05.008

20. Z. Guo, S. Yang, J. Wang, Global exponential synchronization of multiple memristive neural networks with time delay via nonlinear coupling, *IEEE Trans. Neural Netw. Learn. Syst.*, **26** (2015), 1300–1311. https://doi.org/10.1109/TNNLS.2014.2354432

21. C. Xie, Y. Xu, D. Tong, Synchronization of time varying delayed complex networks via impulsive control, *Optik*, **125** (2014), 3781–3787. https://doi.org/10.1016/j.ijleo.2014.01.185

22. Z. Xu, X. Li, P. Duan, Synchronization of complex networks with time-varying delay of unknown bound via delayed impulsive control, *Neural Netw.*, **125** (2020), 224–232. https://doi.org/10.1016/j.neunet.2020.02.003

23. K. Zhang, B. Gharesifard, E. Braverman, Event-triggered control for nonlinear time-delay systems, *IEEE Trans. Autom. Control*, **67** (2021), 1031–1037.

24. B. Liu, T. Liu, P. Xiao, Dynamic event-triggered intermittent control for stabilization of delayed dynamical systems, *Automatica*, **149** (2023), 110847. https://doi.org/10.1016/j.automatica.2022.110847

25. H. Zhou, S. Li, C. Zhang, Synchronization of hybrid switching diffusions delayed networks via stochastic event-triggered control, *Neural Netw.*, **159** (2023), 1–13. https://doi.org/10.1016/j.neunet.2022.11.034

26. X. Liu, T. Chen, Synchronization of nonlinear coupled networks via aperiodically intermittent pinning control, *IEEE Trans. Neural Netw. Learn. Syst.*, **26** (2014), 113–126.

27. J. Lu, D. W. C. Ho, J. Cao, A unified synchronization criterion for impulsive dynamical networks, *Automatica*, **46** (2010), 1215–1221. https://doi.org/10.1016/j.automatica.2010.04.005

28. X. Li, C. Zhu, Saturated impulsive control of nonlinear systems with applications, *Automatica*, **142** (2022), 110375. https://doi.org/10.1016/j.automatica.2022.110375

29. D. Xuan, Z. Tang, J. Feng, J. H. Park, Cluster synchronization of nonlinearly coupled lur'e networks: Delayed impulsive adaptive control protocols, *Chaos Solitons Fract.*, **152** (2021), 111337. https://doi.org/10.1016/j.chaos.2021.111337

30. Z. Wu, J. Pei, X. Zhang, J. Tao, R. Lu, Fuzzy adaptive event-triggered synchronization of complex dynamical networks via switched pinning control, *Inform. Sci.*, **649** (2023), 119674. https://doi.org/10.1016/j.ins.2023.119674

31. X. Wang, J. A. Wang, Q. Sun, X. Wen, J. Zhang, Synchronization of nonlinear coupled complex network via event-dependent intermittent pinning control, *Eur. J. Control*, **69** (2023), 100757. https://doi.org/10.1016/j.ejcon.2022.100757

32. L. Meng, H. Bao, Synchronization of delayed complex dynamical networks with actuator failure by event-triggered pinning control, *Phys. A*, **606** (2022), 128138. https://doi.org/10.1016/j.physa.2022.128138

33. J. Lu, D. W. C. Ho, J. Cao, J. Kurths, Single impulsive controller for globally exponential synchronization of dynamical networks, *Nonlinear Anal. Real World Appl.*, **14** (2013), 581–593. https://doi.org/10.1016/j.nonrwa.2012.07.018

AIMS Press